

STATUS OF THE HARD X-RAY SELF-SEEDING PROJECT AT THE EUROPEAN XFEL

X. Dong, G. Geloni*, S. Karabekyan, L. Samoylova, S. Serkez, H. Sinn,
European XFEL, Schenefeld, Germany
W. Decking, C. Engling, N. Golubeva, V. Kocharyan,
B. Krause, S. Lederer, S. Liu, A. Petrov, E. Saldin, T. Wohlenberg,
DESY, Hamburg, Germany
D. Shu, ANL, Argonne, USA
V. D. Blank, S. Terentiev, TISNCM, Troitsk, Russian Federation

Abstract

A Hard X-ray Self-Seeding setup is currently under realization at the European XFEL, and will be ready for installation in 2018. The setup consists of two single-crystal monochromators that will be installed at the SASE2 undulator line. In this contribution, after a short summary of the physical principles and of the design, we will discuss the present status of the project including both electron beam and X-ray optics hardware. We will also briefly discuss the expected performance of the setup, which should produce nearly Fourier-limited pulses of X-ray radiation with increased brightness compared to the baseline of the European XFEL, as well as possible complementary uses of the two electron chicanes.

THE HARD X-RAY SELF-SEEDING PROJECT AT THE EUROPEAN XFEL

Hard X-ray Self-Seeding (HXRSS) setups based on single-crystal monochromators [1] are active filtering systems allowing for the production of nearly Fourier-limited Hard X-ray radiation pulses at XFELs. They take advantage of the specific impulse response function of single thin crystals in transmission geometry, usually diamond crystals with a thickness around 100 μm , which is constituted by a first response similar to a Dirac δ -function followed by a long tail. The principle was first demonstrated at the LCLS [2].

A Hard X-ray Self-Seeding setup is currently under realization at the European XFEL, and will be ready for installation in 2018.

Double-Chicane Design and Performance

The specific characteristics of the European XFEL, compared to other XFELs, are the high-repetition rate and the availability of long, variable-gap undulators [3]. The latter allows for efficient tapering of the self-seeded signal, and the former for an increase of the average signal brightness, compared to low repetition-rate machines.

In order to increase the signal-to-noise ratio between seed signal and competing SASE (which constitutes, in this case, noise) we rely on a double magnetic chicane design, as sketched in Fig. 1.

We illustrate the advantages of the double-chicane design in Fig. 2, in which we show the filtering stages, Stage 2 and Stage 4, where the C004 reflection from a 100 μm -thick diamond crystal, symmetrically cut, is used. The two undulator parts in Stage 1 and Stage 3 have the same magnetic length. As it can be seen, Stage 4 suffers from poor signal-to-noise ratio. If one proceed with amplification, the seed signal would be lost due to a rapidly growing SASE signal. However, at the filtering position the signal is still almost Fourier limited and therefore the spectral density is higher than that at Stage 2. As a result, the seed signal in the time-domain is larger in Stage 4, compared to Stage 2 of a factor about equal to the ratio between the SASE and the seeded signal bandwidths. The scheme will therefore be highly beneficial in the increase of the signal-to-noise ratio of the seed.

Crystal reflections are available starting from about 3 keV, and although heat loading will likely limit the repetition rate at these very low seed energies, the double-chicane setup will help to improve the situation (see the next subsection). Simulations show that reaching to 14.4 keV should be possible on the high-energy side of the spectrum. The long undulators available at the European XFEL allow for increasing the final output power via tapering. The energy-range around 9 keV is expected to yield optimal performance. Previous studies [4] show that, for a nominal 250 pC electron beam (calculated by s2e simulations [5]) at 17.5 GeV electron energy, combining seeding and tapering one could obtain TW class beams with about 1eV bandwidth, with $7 \cdot 10^{12}$ photons per pulse. Owing to the high-repetition rate of the European XFEL, an average spectral flux of about $2 \cdot 10^{14}$ ph/s/meV can be expected.

Heat Loading Issues

The high-repetition rate of the European XFEL is also related with an increase of heat-loading of the crystals because of impinging X-rays due both to spontaneous emission and SASE/seeded radiation pulses. For both cases, the burst pattern of the European XFEL will lead to a steady temperature increase during a given bunch train, followed by a temperature decrease between one train and the next. If the temperature increase is associated to a shift of the seed frequency of the crystal well beyond a Darwin width, an overall deterioration of the bandwidth is to be expected.

* gianluca.geloni@xfel.eu

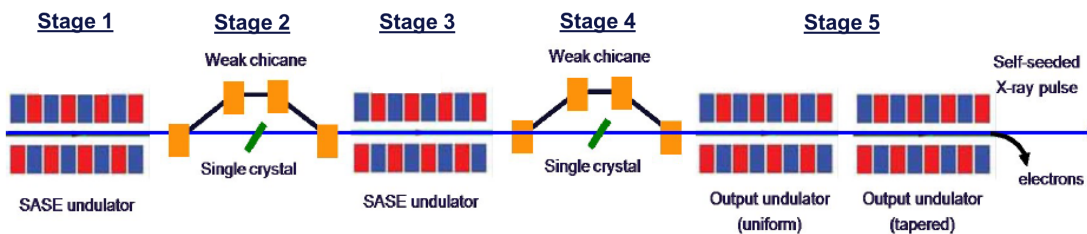


Figure 1: Layout of the HXRSS system being built at the European XFEL.

CHICANE SYSTEM

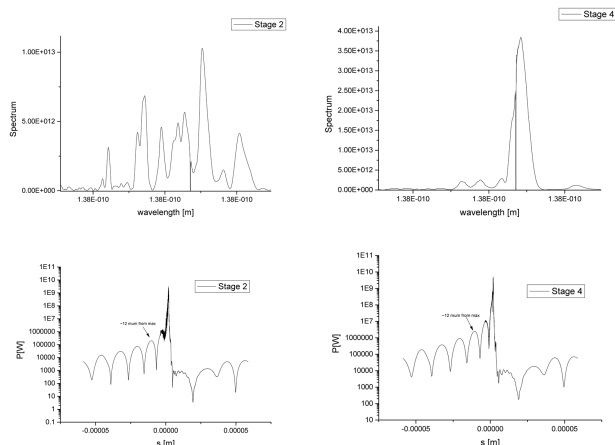


Figure 2: Illustration of the signal-to-noise ratio increase through the double-chicane design. At Stage 4, the spectrum has a bad signal-to-noise ratio, but the maximum spectral density is higher than in the SASE case in Stage 2.

The double-chicane scheme, by increasing the signal-to-noise-ratio, can be used to ease the heat-loading from the SASE/seeding signals. The SASE/seeding component of the heat load depends on the fundamental frequency. For example, for a 100 μm -thick diamond crystal, C004 symmetric reflection at a fundamental energy of 8 keV, a seed frequency-shift equivalent to the Darwin width is to be expected, after 1000 pulses at 4.5 MHz frequency, for an incident energy per pulse of about 3 μJ , corresponding to about 0.7 μJ absorbed energy. However, at 3.3 keV, the energy absorbed by the crystal increases to about 90% of the incident energy, and the same effect is to be expected for an incident pulse energy of about 0.8 μJ . The actual spectral width will be several times larger than the Darwin width so that one can tolerate impinging energies several times larger than those discussed here, i.e. up to several μJ of absorbed energy even for the lowest photon energies: under these conditions, the double-chicane scheme could allow for successful seeding even around 3 keV. However, the double-chicane cannot help dealing with the heat-loading from the spontaneous signal, which is basically independent of the fundamental, and is characterized by a broad spectrum. A pitch oscillator is under study to deal with this issue, which should compensate for the temperature cycle during the pulse train by oscillating the Bragg angle.

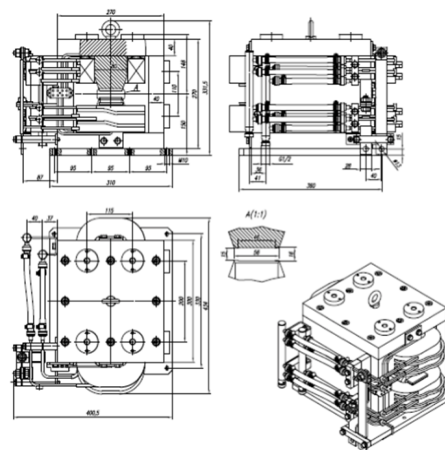


Figure 3: Schematics of the H-magnet dipole used for the HXRSS magnetic chicane.

The chicane system of the HXRSS system at the European XFEL is based on *H*-type dipole magnets, Fig. 3, which have now been fabricated. Two full chicane systems, including the girders, Fig. 4, excluding the monochromators, are presently ready for installation.

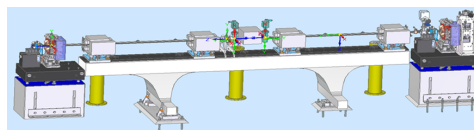


Figure 4: Illustration of the HXRSS chicane system, including girder.

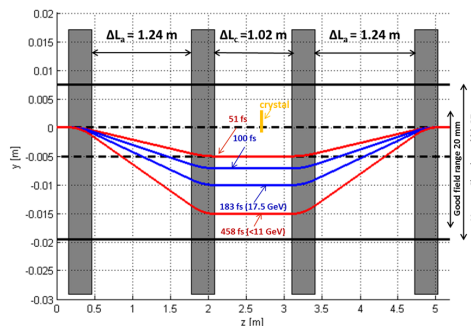


Figure 5: Relation between magnetic delay, electron trajectory and transverse offset in the HXRSS chicane system.

The chicane geometry, and the relation between magnetic delay, electron trajectory and transverse offset in the HXRSS chicane system are summarised in Fig. 5.

Content from this work may be used under the terms of the CC BY 3.0 licence (© 2018). Any distribution of this work must maintain attribution to the author(s), title of the work, publisher, and DOI.

Delay Steps and Autocorrelator Option

We designed the power supply, in terms of resolution and stability, in such a way that the minimum delay step achievable amounts to about 0.1 fs. This enables the use of the chicanes as autocorrelators [6].

Maximum Delay and Multi-Color Option

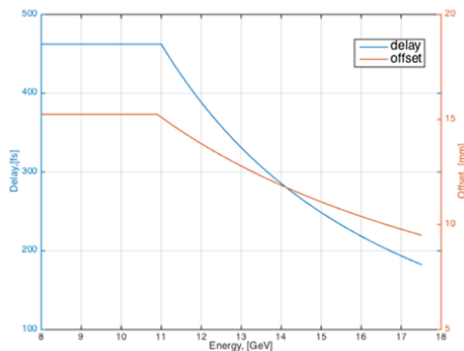


Figure 6: Maximum delay and transverse offset attainable with the European XFEL HXRSS chicane system as a function of the electron energy.

During the chicane design we took care of implementing the largest possible delay in order to enable multiple-color experiments once the HXRSS crystals are retracted [7–9]. Fig. 6 shows the dependence of maximum delay and transverse offset as a function of the electron energy. Up to about 12 GeV one chicane will be able to produce two-color pulses with a maximum temporal separation of about 460 fs.

Minimum Delay and Halo Studies

Finally, it is important to remark that the seed power level is strictly related with the minimum delay that can be achieved, which is in turn linked to the minimum offset between the crystal and the electron that can be tolerated. Beam halo studies, which were reported elsewhere [10] indicate that a minimal offset of about 2 mm is achievable, corresponding to less than 20 fs delay that is optimal for seeding.

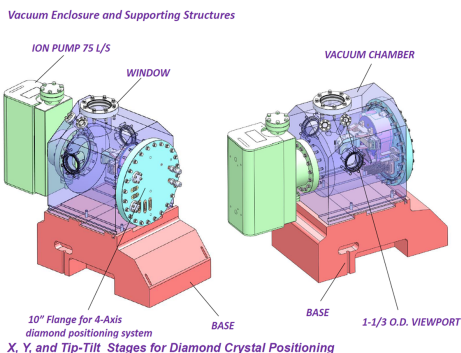


Figure 7: The monochromator system for the European XFEL HXRSS setup: vacuum enclosure and supporting structure.

4-Axis diamond positioning system for LCLS HXRSS monochromator

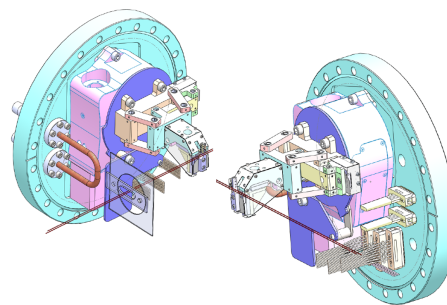


Figure 8: The monochromator system for the European XFEL HXRSS setup: 4-axis diamond positioning system

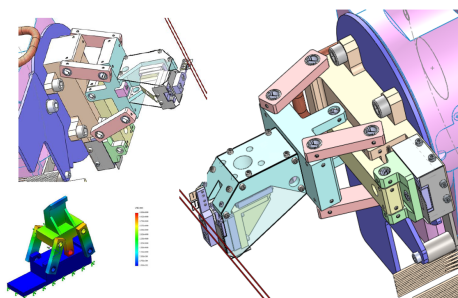


Figure 9: The monochromator system for the European XFEL HXRSS setup: X, Y and tip-tilt stages for the diamond positioning system.

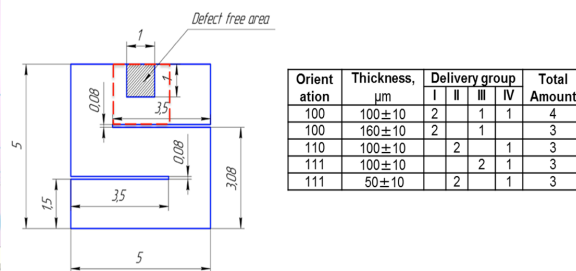


Figure 10: The monochromator system for the European XFEL HXRSS setup: crystal specifications.

MONOCHROMATOR SYSTEM AND CRYSTAL

The monochromator system for the European XFEL has been designed, and two chambers will be ready for installation by 2018. We show in graphic form the vacuum enclosure and the supporting structures, Fig. 7, the 4-axis diamond positioning system, Fig. 8, and the X, Y and tip-tilt stages for the diamond positioning system, Fig. 9. The diamond holder will be capable of hosting two crystals. Several crystals, with variable thicknesses and cuts will be available, Fig. 10.

REFERENCES

- [1] G. Geloni, V. Kocharyan, and E. Saldin, “A novel Self-seeding scheme for hard X-ray FELs”, *Journal of Modern Optics*, vol. 58, issue 16, pp. 1391-1403, 2011.
- [2] J. Amann *et al.*, “Demonstration of self-seeding in a hard X-ray free-electron laser”, *Nature Photonics*, vol. 6, p. 693, 2012.
- [3] M. Altarelli *et al.*, eds, “The European X-ray Free-Electron Laser: Technical Design Report” available at <http://www.xfel.eu/en/documents/>, 2006.
- [4] O. Chubar, G. Geloni, V. Kocharyan *et al.*, “Ultra-high-resolution inelastic X-ray scattering at high-repetition-rate self-seeded X-ray free-electron lasers”, *J. Synchrotron Radiat.*, 23, 410-424, 2016
- [5] I. Zagorodnov, <http://www.desy.de/felbeam/s2e/xfel.html.url>
- [6] G. Geloni, V. Kocharyan, and E. Saldin, “Ultrafast X-ray pulse measurement method”, DESY 10-008, available at <https://arxiv.org/abs/1001.3544>, 2010.
- [7] G. Geloni, V. Kocharyan, and E. Saldin, “Scheme for femtosecond-resolution pump-probe experiments at XFELs with two-color ten GW-level X-ray pulses”, DESY 10-004, available at <https://arxiv.org/abs/1001.3510>, 2010.
- [8] A. A. Lutman *et al.*, “Experimental Demonstration of Femtosecond Two-Color X-Ray Free-Electron Lasers”, *Phys. Rev. Lett.* 110, 13, 2013.
- [9] T. Hara *et al.*, “Two-colour hard X-ray free-electron laser with wide tunability”, *Nat. Commun.* 4, 2919, 2013.
- [10] S. Liu, W. Decking, and L. Fröhlich, “Beam Loss Simulations for the Implementation of the Hard X-Ray Self-Seeding System at European XFEL”, in *Proc. 8th Int. Particle Accelerator Conf. (IPAC'17)*, Copenhagen, Denmark, May 2017, paper WEPAB020, pp. 2611-2614.